Porphyrin-Based Molecular Architectures for Light Energy Conversion

Taku Hasobe [a] , Hideyuki Murata [a] , Shunichi Fukuzumi [b] & Prashant V. Kamat [c]

[a] School of Materials Science, Japan Advanced Institute of Science and Technology (JAIST), Nomi, Ishikawa, Japan

[b] Department of Material and Life Science, Division of Advanced Science and Biotechnology, Graduate School of Engineering, Osaka University, SORST, Japan Science and Technology Agency (JST), Suita, Osaka, Japan

[c] Notre Dame Radiation Laboratory and Departments of Chemistry & Biochemistry and Chemical & Biomolecular Engineering, University of Notre Dame, Notre Dame, Indiana, USA

Version of record first published: 22 Sep 2010

PLEASE SCROLL DOWN FOR ARTICLE

Taylor & Francis
Taylor & Francis Group

Porphyrin-Based Molecular Architectures for Light Energy Conversion

Taku Hasobe
Hideyuki Murata
School of Materials Science, Japan Advanced Institute of Science
and Technology (JAIST), Nomi, Ishikawa, Japan

Shunichi Fukuzumi
Department of Material and Life Science, Division of Advanced
Science and Biotechnology, Graduate School of Engineering,
Osaka University, SORST, Japan Science and Technology
Agency (JST), Suita, Osaka, Japan

Prashant V. Kamat
Notre Dame Radiation Laboratory and Departments of Chemistry
& Biochemistry and Chemical & Biomolecular Engineering,
University of Notre Dame, Notre Dame, Indiana, USA

We have constructed a series of supramolecular photovoltaic cells composed of multi-porphyrin arrays such as porphyrin-alkanethiolate monolayer protected-gold nanoparticles [$H_2PCnMPC$: n is the number of methylene groups in the spacer], porphyrin dendrimers [D_nP_n], and porphyrin-peptide oligomers [$P(H_2P)_n$] and fullerene (C_{60}) on nanostructured SnO_2 electrodes (OTE/SnO_2). These multi-porphyrin arrays form complexes with fullerene molecules and they form clusters in acetonitrile/toluene mixed solvent. The highly colored composite clusters are assembled as three-dimensional arrays onto nanostructured SnO_2 films [denoted as $OTE/SnO_2/(multi\text{-}porphyrin\ array+C_{60})_m$] using an electrophoretic deposition method. These highly organized molecular assembly films attain drastic enhancement of light energy conversion properties as compared to the non-organized reference system. The maximum power conversion efficiency

(η) *of OTE/SnO$_2$/(H$_2$PC15MPC+C$_{60}$)$_m$ reaches 1.5%, which is 45 times higher than that of the reference system (0.035%).*

INTRODUCTION

Recently, attention has been drawn to develop inexpensive renewable energy sources. Novel approaches for the production of efficient and low-cost organic solar cells are necessary for future development of next generation devices [1–5]. The construction of efficient photovoltaic devices requires an enhanced light-harvesting efficiency of chromophore molecules throughout the solar spectrum together with a highly efficient conversion of the harvested light into electrical energy. In this context, progress is being made in the development of heterojunction organic solar cells, which possess an active layer of a conjugated donor polymer and an acceptor fullerenes [1,4–9].

Fullerene has been used as a suitable electron acceptor component in such organic solar cells, since electron-transfer reduction of C$_{60}$ is highly efficient because of the minimal changes of structure and solvation associated with the electron-transfer reduction [10–12]. In these polymer blends, efficient photoinduced electron transfer occurs at the donor-fullerene interface, and intimate mixing of donor and fullerene acceptor is essential for efficient charge separation. On the other hand, various types of multi-dye assembly systems such as dendrimers and linear oligomers have been developed, attracting considerable interest owing to their unique physical and chemical properties. The first candidate of such components is a porphyrin that is involved in a number of important biological electron transfer systems including the primary photochemical reactions of chlorophylls (porphyrin derivatives) in the photosynthetic reaction centers [13]. Porphyrins contain an extensively conjugated two-dimensional π-system and thus are suitable for efficient electron transfer.

Porphyrin-alkanethiolate monolayer protected-gold nanoclusters with well-defined size (8–9 nm) and spherical shape also exhibit high light-harvesting capability and suppress undesirable energy transfer quenching of the porphyrin singlet excited state by the gold surface relative to the bulk gold [14–16]. Porphyrin dendrimers and porphyrin-peptide oligomers are also good candidates as light collectors, since the antenna function of these multi-porphyrin arrays resembles that of the light harvesting antenna [17,18]. Such pre-organized multi-porphyrin arrays possess a suitable void space between the porphyrin

moieties, which can form supramolecular complexes with the guest fullerene [19–21]. The porphyrin-fullerene interaction energies are reported to be in the range from -16 to $-18\,\mathrm{kcal\,mol}^{-1}$ [22]. A strong interaction between porphyrins and fullerenes is likely to be a good driving force for the formation of supramolecular complexes between porphyrin and C_{60}. Thus, a combination of multi-porphyrin arrays (chromophores and electron donor) and fullerenes (electron acceptor) seems ideal for fulfilling an enhanced light-harvesting efficiency of chromophores throughout the solar spectrum and a highly efficient conversion of the harvested light into the high energy state of the charge separation by photoinduced electron transfer. We report herein novel light energy conversion systems using fullerenes with multi-porphyrin arrays such as porphyrin-alkanethiolate protected gold nanoparticles (H_2PCnMPC: $n = 5, 11, 15$), porphyrin dendrimers (D_nP_n: $n = 4, 8, 16$) and porphyrin-peptide oligomers ($P(H_2P)_n$: $n = 1, 2, 4, 8$) (Fig. 1), which are clusterized on nanostructured SnO_2 electrodes.

EXPERIMENTAL

General

Melting points were recorded on a Yanagimoto micro-melting point apparatus and not corrected. ^{1}H NMR spectra were measured on a JEOL EX-270 (270 MHz) or a JEOL JMN-AL300 (300 MHz). Matrix-assisted laser desorption/ionization (MALDI) time-of-flight mass spectra (TOF) were measured on a Kratos Compact MALDI I (Shimadzu). The UV-visible spectra were recorded on a Shimadzu 3101 spectrophotometer. Transmission electron micrographs (TEM) of C_{60} clusters were recorded by applying a drop of the sample to carbon-coated copper grid. Images were recorded using a Hitachi H600 transmission electron microscope.

Materials

All solvents and chemicals were of reagent grade quality, obtained commercially and used without further purification unless otherwise noted (*vide infra*). Thin-layer chromatography (TLC) and flash column chromatography were performed with Art. 5554 DC-Alufolien Kieselgel 60 F_{254} (Merck), and Fujisilicia BW300, respectively. Nanostructured SnO_2 films were cast on an optically transparent electrode (OTE) by applying a 2% colloidal solution obtained from Alfa Chemicals. The air-dried films were annealed at 673 K. The details of the preparation of SnO_2 films on conducting glass substrate were reported

-Gold Nanoparticle-

-Peptide-Oligomer-

H₂PCnMPC; (*n* = 5, 11, 15)

P(H₂P)ₙ; (*n* = 1 , 2, 4, 8)

-Dendritic Structure-

D₄P₄

D₁₆P₁₆

D₈P₈

H₂P-ref
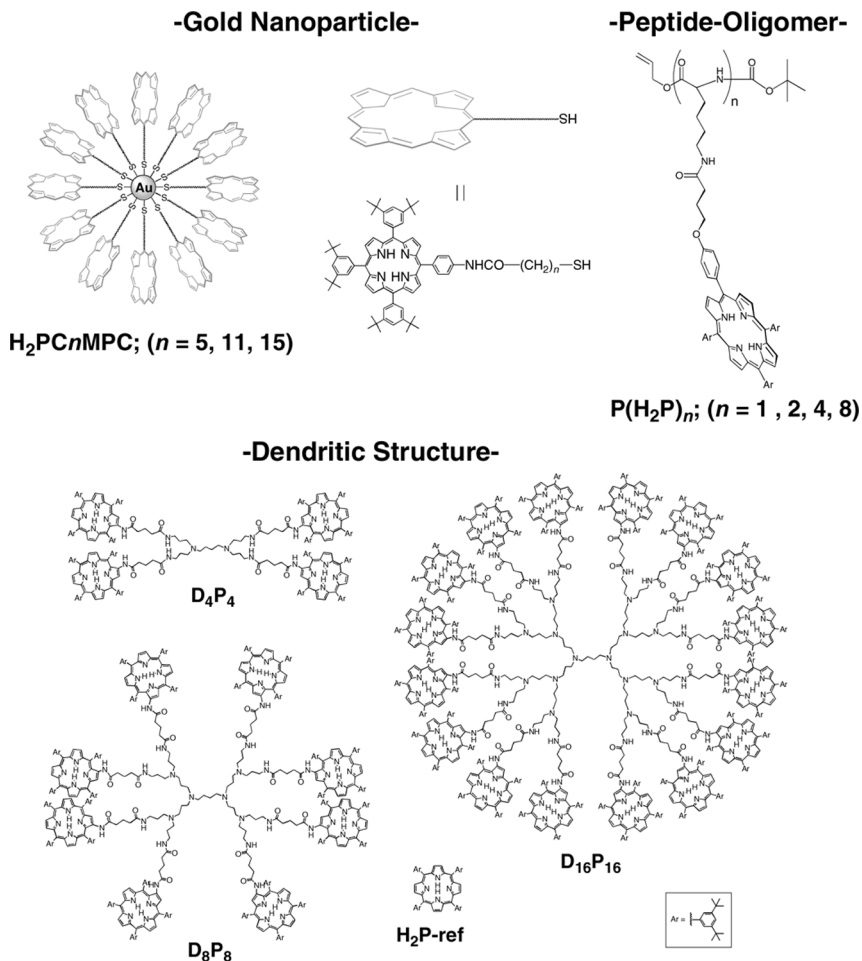
FIGURE 1 Multi-porphyrin arrays used in this study.

elsewhere [15]. The nanostructured SnO_2 film electrode is referred as OTE/SnO_2.

Electrophoretic Deposition of Cluster Films

A known amount of porphyrin derivatives, C_{60} or mixed cluster solution in acetonitrile/toluene (3/1, v/v, 2 mL) was transferred to a 1 cm cuvette in which two electrodes (viz., OTE/SnO_2 and OTE) were kept at a distance of 6 mm using a Teflon spacer. A DC electric field

($\sim$200 V/cm) was applied between these two electrodes using a Fluke 415 power supply. The deposition of the film can be visibly seen as the solution becomes colorless with simultaneous brown coloration of the OTE/SnO$_2$ electrode. The OTE/SnO$_2$ electrode coated with mixed multi-porphyrin array and C$_{60}$ clusters is referred as OTE/SnO$_2$/ (multi-porphyrin array +C$_{60}$)$_m$.

Photoelectrochemical Measurements

Photoelectrochemical measurements were carried out using a working electrode and a Pt gauge counter electrode in the cell assembly using a Keithley model 617 programmable electrometer. The electrolyte was 0.5 M NaI and 0.01 M I$_2$ in acetonitrile. A collimated light beam from a 150 W Xenon lamp with a 400 nm cut-off filter was used for excitation of (multi-porphyrin array +C$_{60}$)$_m$ films deposited on SnO$_2$ electrodes. A Bausch and Lomb high intensity grating monochromator was introduced into the path of the excitation beam for the selected wavelength.

SUPRAMOLUCULA COMPLEX OF PORPHYRINS AND FULLERENES USING GOLD NANOPARTICLES

Figure 2 summarizes the procedure to prepare porphyrin (donor) and fullerene (acceptor) assemblies. First porphyrin-alkanethiolate monolayer protected-gold nanoclusters (H$_2$PCnMPC) of spherical shape (8–9 nm) [16] are prepared starting from porphyrin-alkanethiol. By considering the inner gold core as a sphere (58.01 atoms/nm^3) and an outermost layer of hexagonally close-packed gold atoms (13.89 atoms/nm^2) we estimate the core of H$_2$PC11MPC to contain 280 Au atoms, 143 atoms of which are on the Au surface. Given the values of the elemental analysis of H$_2$PC11MPC (H: 4.88%; C: 44.77%; N: 3.10%), there are 57 porphyrin alkanethiolate chains on gold surface for H$_2$PC11MPC. These nanoparticles form complexes with fullerene molecules (tertiary organization) and they are clusterized in acetonitrile/toluene mixed solvent (quaternary organization). The quaternary organization of H$_2$PCnMPC and C$_{60}$ composite assemblies [denoted as (H$_2$PCnMPC+C$_{60}$)$_m$] was performed by injecting a mixed toluene solution of H$_2$PCnMPC and C$_{60}$ in acetonitrile/toluene (3/1, v/v). This procedure allows us to obtain the clusters of H$_2$PCnMPC and C$_{60}$ complex. The clusters of the H$_2$PCnMPC reference system without C$_{60}$ [denoted as (H$_2$PCnMPC)$_m$] or porphyrin and C$_{60}$ reference system without gold nanoparticles [denoted as (H$_2$P-ref+C$_{60}$)$_m$;
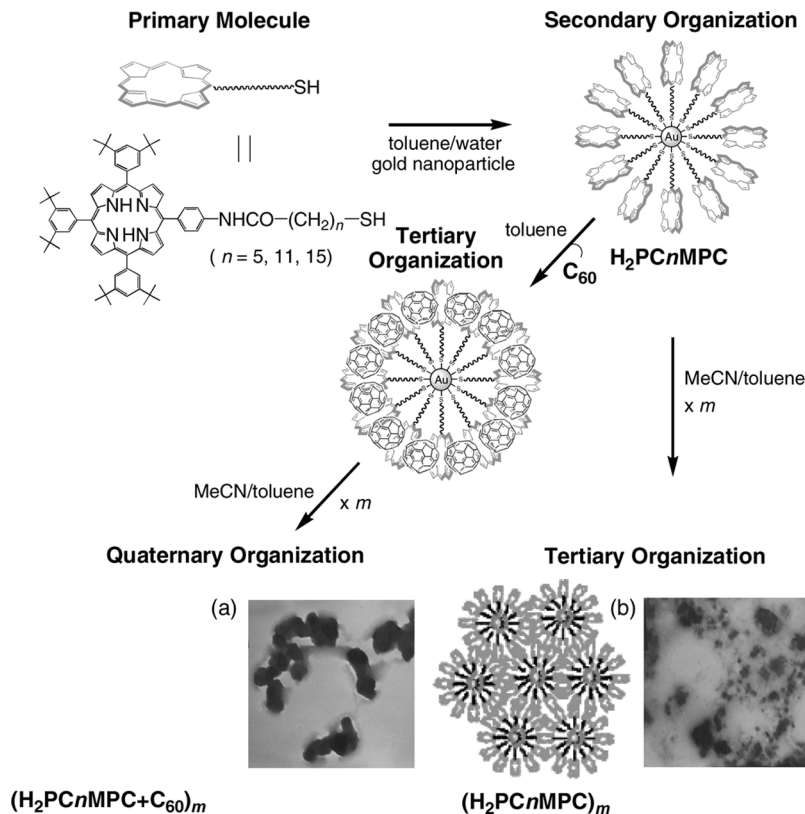
FIGURE 2 Illustration of high order organization between porphyrins and fullerenes in this study. Transmission electron micrograph (TEM) images of (a) $(H_2PC11MPC+C_{60})_m$ and (b) $(H_2PC11MPC)_m$. (From reference 15. Reprinted with the permission of the American Chemical Society)

H_2P-ref: 5,10,15,20-tetrakis(3,5-di-*tert*-butylphenyl)-porphyrin] were also obtained in the same manner.

The absorption spectra of $(H_2PCnMPC+C_{60})_m$ and $(H_2PCnMPC)_m$ in acetonitrile/toluene 3:1 mixture are broader than those in toluene, implying formation of the clusters in the mixed solvent. The broad absorption in the 700–800 nm region is indicative of the charge-transfer absorption band. The π-complex is formed between the porphyrin and C_{60} [15,23]. TEM images of $(H_2PCnMPC+C_{60})_m$ (Fig. 2a) displays well-controlled size and shape of larger nanoclusters with a diameter of 300–400 nm. These clusters are in sharp contrast with the TEM image of $(H_2PC11MPC)_m$ which exhibit irregular, smaller size (Fig. 2b). Judging from the diameter of $H_2PCnMPC$ (8–9 nm), one

can conclude that $H_2PCnMPC$ and C_{60} molecules are self-assembled in the mixed solution to yield large size donor-acceptor (D-A) nano-clusters. By subjecting the resultant cluster suspension to a high electric (DC) field ($\sim 200 \, V \, cm^{-1}$ for 1 min), mixed $H_2PCnMPC$ and C_{60} clusters $[(H_2PCnMPC+C_{60})_m]$, reference clusters $[(H_2PCnMPC)_m$ or $(H_2P\text{-ref}+C_{60})_m]$ are deposited onto an optically transparent electrode (OTE) of nanostructured SnO_2 electrode (OTE/SnO_2) [denoted as $OTE/SnO_2/(H_2PCnMPC+C_{60})_m$, $OTE/SnO_2/(H_2PCnMPC)_m$, and $OTE/SnO_2/(H_2P\text{-ref}+C_{60})_m]$, respectively. These results ensure that incident light is absorbed efficiently in the visible and near infrared regions by $OTE/SnO_2/(H_2PCnMPC+C_{60})_m$. Similar trend is also observed in the case of $H_2PC5MPC$ and $H_2PC15MPC$ [15].

PHOTOVOLTAIC PROPERTIES OF H_2PC_nMPC–C_{60} ASSEMBLIES

To evaluate the photoelectrochemical performance of the $(H_2PCnMPC+C_{60})_m$ films, we used the $OTE/SnO_2/(H_2PCnMPC+C_{60})_m$ electrode as a photoanode in a photoelectrochemical cell. Photocurrent measurements were performed in acetonitrile containing NaI (0.5 M) and I_2 (0.01 M) as redox electrolyte using a Pt gauge counter electrode (Fig. 3) [24]. Photocurrent action spectra of $(H_2PCnMPC+C_{60})_m$ cluster films are shown in Figure 4. The IPCE values were calculated by normalizing the photocurrent values to incident light energy and intensity using Eq. (1), [25]

$$\text{IPCE } (\%) = 100 \times 1240 \times I_{sc}/(I_{inc} \times \lambda) \tag{1}$$

where I_{sc} is the short circuit photocurrent (A/cm^2), I_{inc} is the incident light intensity (W/cm^2), and λ is the wavelength (nm). The overall response of $OTE/SnO_2/(H_2PCnMPC+C_{60})_m$ parallels the broad absorption features, indicating the involvement of both $H_2PCnMPC$ and C_{60} in the photocurrent generation. The concentration effects of C_{60} were investigated by keeping the concentration of H_2PC11-MPC constant. The photocurrent increases with increasing ratio of C_{60}exhibits a maximum IPCE of 28% at 490 nm at a ratio of $[H_2P]:[C_{60}] = 38:62$ [15]. Considering the well-established photodynamics of the porphyrin-fullerene system, the porphyrin excited singlet state is expected to be quenched by C_{60} via electron transfer in the porphyrin-C_{60} complex rather than by the gold nanocluster.

The length of the linker molecule also influenced the IPCE. Figure 4 shows the effect of the alkanethiolate chain length on the IPCE values [15]. The action spectra indicate that the higher IPCE and the broader photoresponse are attained with the longer chain length of $H_2PCnMPC$. In particular, $OTE/SnO_2/(H_2PC15MPC+C_{60})_m$ exhibits
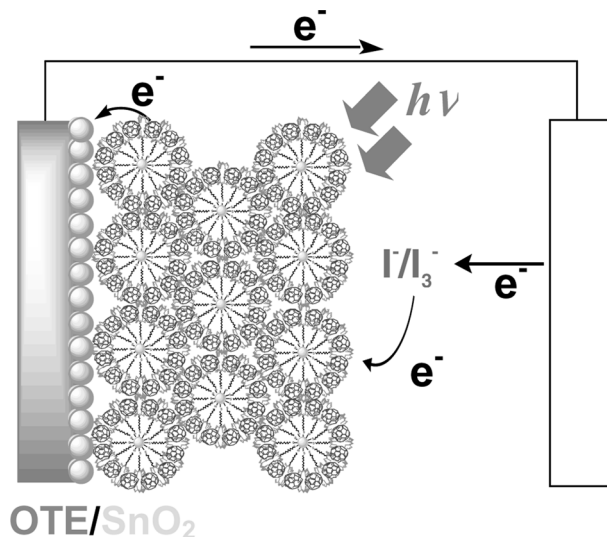
FIGURE 3 Operation of a photochemical solar cell using supramolecular assembly of $H_2PCnMPC$ and C_{60}. (From reference 15. Reprinted with the permission of the American Chemical Society.)

the maximum IPCE value (54%) and very broad photoresponse (up to ~ 1000 nm), thus extending the response to the near IR region. In $OTE/SnO_2/(H_2PC15MPC+C_{60})_m$, a long methylene spacer of $H_2PC15MPC$ allows sufficient space for the insertion of fullerene molecules and interact with the neighboring two porphyrin moieties (see: illustration of insertion of C_{60} between the porphyrin rings of $H_2PC15MPC$ in Fig. 4A).The power conversion efficiency (η) of the photochemical solar cell can be evaluated by varying the load resistance (Fig. 4B) [15]. A drop in the photovoltage and an increase in the photocurrent are observed with decreasing the load resistance. The $OTE/SnO_2/(H_2PC15MPC+C_{60})_m$ system has a much larger fill factor (FF) of 0.43, open circuit voltage (V_{oc}) of 380 mV, short circuit current density (I_{sc}) of 1.0 mA cm^{-2}, and the overall power conversion efficiency (η) of 1.5% at input power (W_{in}) of 11.2 mW cm^{-2} [26].

SOLAR CELLS USING PORPHYRIN DENDRIMERS AND PORPHYRIN-PEPTIDE OLIGOMERS

We have also constructed supramolecular photovoltaic cells based on porphyrin dendrimers $[D_nP_n]$ and porphyrin peptide oligomers $[P(H_2P)_n]$ by using the strategy described in the previous section.

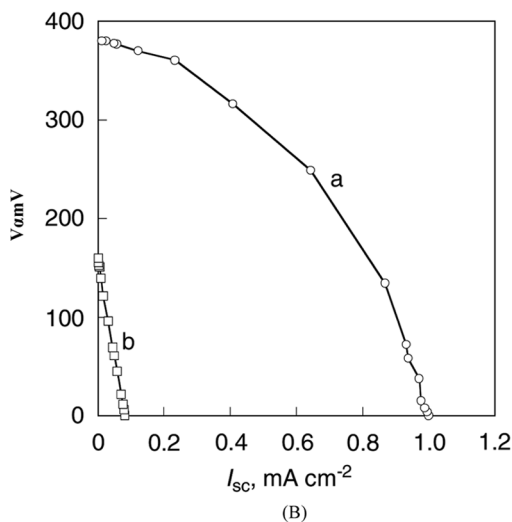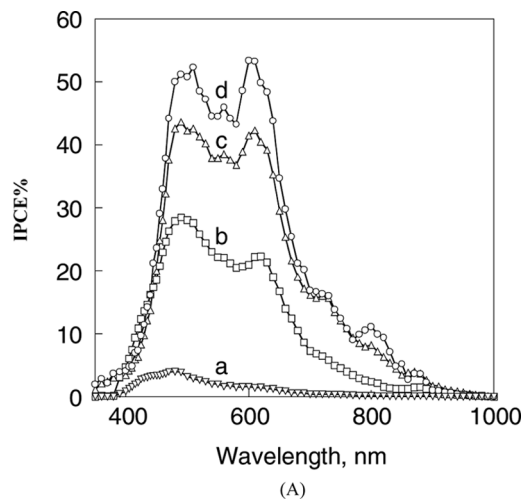**FIGURE 4** (A) Photocurrent action spectra of $OTE/SnO_2/(H_2PCnMPC+ C_{60})_m$ electrode($[H_2P] = 0.19$ mM; (a) $n = 5$, $[C_{60}] = 0.31$ mM; (b) $n = 11$, $[C_{60}] = 0.31$ mM; (c) $n = 15$, $[C_{60}] = 0.31$ mM; (d) $n = 15$, $[C_{60}] = 0.38$ mM. Electrolyte; 0.5 M NaI and 0.01 M I_2 in acetonitrile. The insertion shows a detail structure of supramolecular complex of $H_2PCnMPC$-C_{60} assembly between porphyrin and fullerene. (B) Current–Voltage characteristics of (a) $OTE/SnO_2/(H_2PC15MPC+C_{60})_m$ electrode and (b) $OTE/SnO_2/(H_2Pref+C_{60})_m$ electrode prepared from cluster solution of ($[H_2P] = 0.19$ mM; $[C_{60}] = 0.38$ mM) under visible light illumination ($\lambda > 400$ nm); electrolyte 0.5 M NaI and 0.01 M I_2 in acetonitrile; input power: 11.2 mW/cm^2. (From reference 15. Reprinted with the permission of the American Chemical Society.)
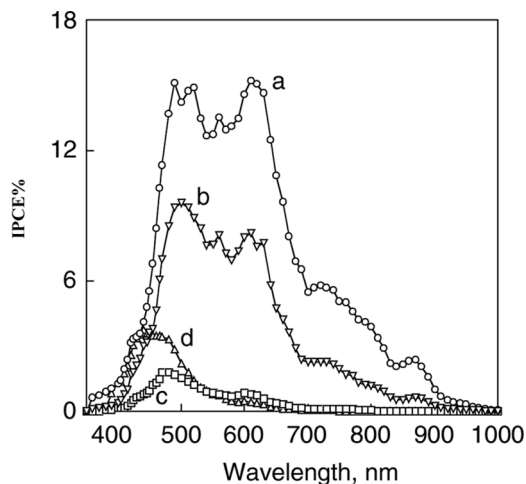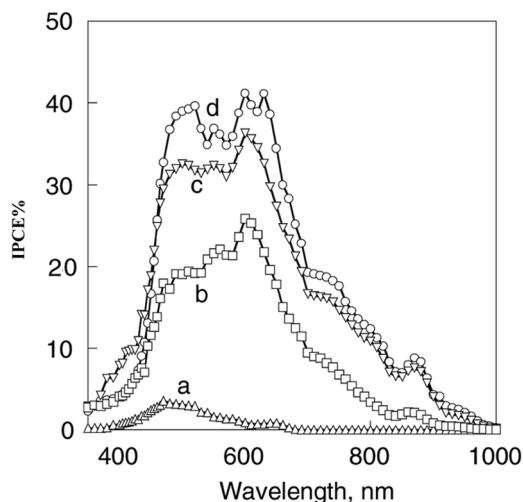
FIGURE 5 (A) The photocurrent action spectra (IPCE vs. wavelength) of $OTE/SnO_2/(D_nP_n+C_{60})_m$ and $OTE/SnO_2/(H_2P\text{-ref}+C_{60})_m$ under short circuit conditions. (a) $[D_4P_4] = 0.048$ mM, (b) $[D_8P_8] = 0.024$ mM, (c) $[D_{16}P_{16}] = 0.012$ mM, and (d) $[H_2P\text{-ref}] = 0.19$ mM; $[C_{60}] = 0.31$ mM. (B) The photocurrent action spectra (IPCE vs. wavelength) of $OTE/SnO_2/(P(H_2P)_n+C_{60})_m$ (a) $[P(H_2P)_1] = 0.19$ mM, (b) $[P(H_2P)_2] = 0.10$ mM, (c) $[P(H_2P)_4] = 0.048$ mM, and (d) $[P(H_2P)_8] = 0.024$ mM; $[C_{60}] = 0.31$ mM in acetonitrile/toluene $= 3/1$. Electrolyte; 0.5 M NaI and 0.01 M I_2 in acetonitrile. (From reference 17 and 18. Reprinted with the permission of the American Chemical Society and Wiley-VCH.)

Figure 5A shows the wavelength dependence of the IPCE spectra of the $OTE/SnO_2/(D_nP_n+C_{60})_m$ system and the reference system ($OTE/SnO_2/(H_2P\text{-ref}+C_{60})_m$). The $OTE/SnO_2/(D_4P_4+C_{60})_m$ system (spectrum a in Fig. 5A) exhibits maximum IPCE value of 15%. The broad photoresponse extends well into the infrared and contrasts narrow response of the reference system (spectrum d) [18]. The action spectra in the long wavelength region (e.g., the peak around 880 nm in Fig. 5A) results from the charge-transfer interaction of the porphyrins and C_{60}. Such an effective photoenergy conversion is ascribed to the dendritic structure that controls three-dimensional organization between porphyrin and C_{60}. However, the IPCE value decreases with increasing the number of dendrimer generation and the $OTE/SnO_2/(D_{16}P_{16}+C_{60})_m$ system (spectrum c in Fig. 5A) has even smaller IPCE value compared with the reference system [$OTE/SnO_2/(H_2P\text{-ref}+C_{60})_m$] (spectrum d in Fig. 5A). The 'rigid' structure of porphyrin dendrimers, is likely to hamper effective interaction between the porphyrin units and C_{60} in the higher dendritic generation. Such 'rigid' structures also have an effect on electron or hole-transport properties on the thin film.

In contrast with porphyrin dendrimers, IPCE values of solar cells constructed with porphyrin-peptide oligomers [$OTE/SnO_2/(P(H_2P)_n+C_{60})_m$: ($n = 1, 2, 4, 8$)] exhibit a increase in IPCE with increasing number of porphyrins in a polypeptide unit. The $OTE/SnO_2/(P(H_2P)_8+C_{60})_m$ system has the maximum IPCE value of 42% at 600 nm the broad photoresponse extends into the infrared region (up to 1000 nm) [17]. These results suggest that the electron-transfer properties of polypeptide based donor-acceptor assemblies can be improved by increasing the number of porphyrins in a polypeptide unit. The overall power conversion efficiency (η) of 1.3% at input power (W_{in}) of 3.4 mW cm^{-2} [27]. The I/V characteristics of $OTE/SnO_2/(P(H_2P)_8+C_{60})_m$ system is also remarkably enhanced (more than 30 times) as compared with the $OTE/SnO_2/(P(H_2P)_1+C_{60})_m$ electrode ($\eta = 0.043\%$) under the same experimental conditions.

PHOTOCURRENT GENERATION MECHANISM

The photocurrent generation is initiated by the photoinduced charge separation from the porphyrin singlet excited state ($^1H_2P^*/H_2P^{\bullet+} = -0.7$ V vs NHE) to C_{60} ($C_{60}/C_{60}^{\bullet-} = -0.2$ V vs NHE) in the porphyrin-C_{60} supramolecular complex rather than direct electron injection to the conduction band of SnO_2 (0 V vs NHE) system, which is energetically more favorable (vide infra). The electron transfer from $^1H_2P^*$ to C_{60} competes well with the energy transfer to the gold

nanoparticles [24]. While the reduced C_{60} injects electrons into the SnO_2 nanocrystallites, the oxidized porphyrin ($H_2P/H_2P^{\bullet+} = 1.2\,V$ vs NHE) undergoes the electron transfer reduction with iodide ion ($I_3^-/I^- = 0.5\,V$ vs NHE) in the electrolyte [24].

SUMMARY

Highly organized supramolecular architectures of multi-porphyrin arrays with fullerenes provide new ways to improve light-harvesting efficiency of donor-acceptor based supramolecular assemblies. Absorption of the incident light throughout the solar spectrum results in the efficient charge separation. There are two essential factors for efficient light energy conversion in donor-acceptor based photochemical systems. First one is the charge separation between porphyrin and fullerene, and the other one is the transport of charge carriers in the thin film. Three-dimensional steric control of porphyrin and fullerene in the supramolecular systems contributes to both these factors. Systems based on supramolecular approach have promising perspective for the development of efficient light energy conversion devices.

REFERENCES

[1] Ma, W., Yang, C., Gong, X., Lee, K., & Heeger, A. J. (2005). *Adv. Funct. Mater.*, *15*, 1617.
[2] Bach, U., Lupo, D., Comte, P., Moser, J. E., Weissortel, F., Salbeck, J., Spreitzer, H., & Gratzel, M. (1998). *Nature*, *395*, 583.
[3] O'Regan, B. & Gratzel, M. (1991). *Nature*, *353*, 737.
[4] Padinger, F., Rittberger, R. S., & Sariciftci, N. S. (2003). *Adv. Funct. Mater.*, *13*, 85.
[5] Shaheen, S. E., Brabec, C. J., Sariciftci, N. S., Padinger, F., Fromherz, T., & Hummelen, J. C. (2001). *Appl. Phys. Lett.*, *76*, 841.
[6] Yu, G., Gao, J., Hummelen, J. C., Wudl, F., & Heeger, A. J. (1995). *Science*, *270*, 1789.
[7] Wienk, M. M., Kroon, J. M., Verhees, W. J. H., Knol, J., Hummelen, J. C., van Hal, P. A., & Janssen, R. A. J. (2003). *Angew. Chem., Int. Ed.*, *42*, 3371.
[8] Granstrom, M., Petritsch, K., Arias, A. C., Lux, A., Andersson, M. R., & Friend, R. H. (1998). *Nature*, *395*, 257.
[9] Mutolo, K. L., Mayo, E. I., Rand, B. P., Forrest, S. R., & Thompson, M. E. (2006). *J. Am. Chem. Soc.*, *128*, 8108.
[10] Imahori, H., Yamada, H., Guldi, D. M., Endo, Y., Shimomura, A., Kundu, S., Yamada, K., Okada, T., Sakata, Y., & Fukuzumi, S. (2002). *Angew. Chem., Int. Ed.*, *41*, 2344.
[11] Fukuzumi, S. (2006). *Bull. Chem. Soc. Jpn.*, *79*, 177.
[12] Fukuzumi, S. (2003). *Pure Appl. Chem.*, *75*, 577.
[13] Gust, D., Moore, T. A., & Moore, A. L. (1993). *Acc. Chem. Res.*, *26*, 198.
[14] Hasobe, T., Imahori, H., Fukuzumi, S., & Kamat, P. V. (2003). *J. Am. Chem. Soc.*, *125*, 14962.
[15] Hasobe, T., Imahori, H., Kamat, P. V., Ahn, T. K., Kim, S. K., Kim, D., Fujimoto, A., Hirakawa, T., & Fukuzumi, S. (2005). *J. Am. Chem. Soc.*, *127*, 1216.

[16] Imahori, H., Arimura, M., Hanada, T., Nishimura, Y., Yamazaki, I., Sakata, Y., & Fukuzumi, S. (2001). *J. Am. Chem. Soc.*, *123*, 335.

[17] Hasobe, T., Kamat, P. V., Troiani, V., Solladie, N., Ahn, T. K., Kim, S. K., Kim, D., Kongkanand, A., Kuwabata, S., & Fukuzumi, S. (2005). *J. Phys. Chem. B*, *109*, 19.

[18] Hasobe, T., Kashiwagi, Y., Absalom, M. A., Hosomizu, K., Crossley, M. J., Imahori, H., Kamat, P. V., & Fukuzumi, S. (2004). *Adv. Mater.*, *16*, 975.

[19] Boyd, P. D. W. & Reed, C. A. (2005). *Acc. Chem. Res.*, *38*, 235.

[20] Olmstead, M. M., Costa, D. A., Maitra, K., Noll, B. C., Phillips, S. L., Van Calcar, P. M., & Balch, A. L. (1999). *J. Am. Chem. Soc.*, *121*, 7090.

[21] Tashiro, K., Aida, T., Zheng, J. Y., Kinbara, K., Saigo, K., Sakamoto, S., & Yamaguchi, K. (1999). *J. Am. Chem. Soc.*, *121*, 9477.

[22] Sun, D., Tham, F. S., Reed, C. A., Chaker, L., & Boyd, P. D. W. (2002). *J. Am. Chem. Soc.*, *124*, 6604.

[23] Tkachenko, N. V., Lemmetyinen, H., Sonoda, J., Ohkubo, K., Sato, T., Imahori, H., & Fukuzumi, S. (2003). *J. Phys. Chem. A*, *107*, 8834.

[24] Hasobe, T., Imahori, H., Fukuzumi, S., & Kamat, P. V. (2003). *J. Phys. Chem. B*, *107*, 12105.

[25] Hasobe, T., Imahori, H., Fukuzumi, S., & Kamat, P. V. (2003). *J. Mater. Chem.*, *13*, 2515.

[26] η value of OTE/SnO$_2$/(H$_2$PC15MPC+C$_{60}$)$_m$ system is $\sim$0.7% at input power (W_{in}) of 100 mW cm^{-2}.

[27] η value of OTE/SnO$_2$/(P(H$_2$P)$_8$+C$_{60}$)$_m$ system is 0.65% at input power (W_{in}) of 100 mW cm^{-2}.